Study on validation method of visible imagery spatial resolution of imager on geostationary platform

Qiang Guo (郭 强)[1,2]

[1]*Key Laboratory of Radiometric Calibration and Validation for Environmental Satellites, China Meteorological Administration, Beijing 100081*

[2]*National Satellite Meteorological Center, China Meteorological Administration, Beijing 100081*

Received December 5, 2005

Based on the analysis for the main elements of the total modulation transfer function (MTF) of imager on geostationary platform, the precise evaluation for its low spatial frequency spectrum has been achieved. Meanwhile, it is pointed out that the main cause of imagery spatial resolution lower than the designed value is the "slight defocus" of imager focal plane array (FPA). The validation method for visible imagery spatial resolution is proposed based on the analysis of defocused optical system model and edge-spread-function (ESF), the relative error is less than 7% after alleviating stray light effects. This method has been applied in the in-orbit ground testing of FY-2C geostationary meteorological satellite successfully.

OCIS codes: 110.3000, 100.2960, 080.2740, 120.0280.

For an imaging instrument, such as imager, it is feasible to validate its spatial resolution by means of image processing. According to the definition of instrument spatial resolution, it is applied successfully in polar platforms, such as SPOT of France and ROCAT of Taiwan, China[1], by choosing the pre-disposed high-contrast objects in the pass-way of satellite and then retrieving the modulation transfer function (MTF)[2]. In domestic, an indirect evaluation method was proposed based on varied information entropy[3], whose authenticity and validity are still uncertain and should be analyzed more. On the other hand, for an imager in geostationary platform, it is impossible to dispose some special objects for testing and validating because the highest spatial resolution is only 1 km among all satellites in these platforms and their nadir positions are almost in oceans. However, geostationary operational environmental satellite (GOES) imager scans the lunar edge to get its exact profile, and then uses the pre-launched MTF testing results to modify the retrieval errors in higher spatial frequency spectrum[4]. The retrieved MTF is applied to improve the quality of imagery by means of de-convolution[5].

In need of engineering application requirements, based on analysis of the main elements of imager MTF in-orbit, the primary low spatial frequency spectrum is evaluated precisely using the special profile of ground objects near the nadir point. Meanwhile, combined with the analyzed results for the defocused model of ideal optical system, it is clarified that the main reason for the real spatial resolution lower than that of standard is slight defocus of focal plane array (FPA) caused by strong shakes during satellite launch. Also, the in-orbit validation method of visible imagery spatial resolution of imager is proposed.

Here, two basic conceptions will be interpreted. The first one is instrument spatial resolution which represents the capability of recognizing and classifying different objects according to geometric characteristics, it is usually expressed with instant field-of-view (IFOV). For imager, IFOV will influence its imaging performance. The second one is imagery spatial resolution which can be understood that, for a given imagery, if there are some pixels corresponding to a detectable target, which can be distinguished effectively from the background, its minimum size is the imagery spatial resolution[6].

From the classical theory of instrument designing, the spatial resolution depends on the cut-off spatial frequency of total MTF completely, and it consists of four main factors, the MTF of optical system ($\mathrm{MTF_o}$), the spatial and temporal filter functions of detector ($\mathrm{DTF_s}$, $\mathrm{DTF_t}$), and the transfer function of electronic system (LTF), which are satisfied with

$$\mathrm{MTF_{total}} = \mathrm{MTF_o}\cdot\mathrm{DTF_s}\cdot\mathrm{DTF_t}\cdot\mathrm{LTF} = \mathrm{MTF_o}\cdot\mathrm{DTF_s}\cdot\frac{1}{1+\left(\frac{f}{f_0}\right)^2}, \quad (1)$$

where f_0 is the eigen-frequency at the half-power-point of electronic system. Here, it is assumed that the electronic bandwidth is enough, so Eq. (1) can be simplified as

$$\mathrm{MTF_{total}} \approx \mathrm{MTF_o}\cdot\mathrm{DTF_s}, \quad (2)$$

Equation (2) shows that $\mathrm{MTF_{total}}$ is determined by the optical system and detector mainly.

Optical transfer function (OTF) can be calculated from point-spread-function (PSF) using Fourier transforms, and its norm is MTF. Obviously, if an image of point-target can be found in acquired imageries, the MTF could be calculated using above equations. However, because of influence of noise and jams, it is hardly to achieve. So, the alternative way is to search a "smooth" knife-edge in imageries. However, when an imager can be considered as a linear shift invariant (LSI) system, a real smooth knife-edge target could be regarded as a step input signal and the knife-edge image can be treated as the output of imager response. The relationship meets

$$\mathrm{STEP}(f_x)\cdot\mathrm{OTF_{total}}(f_x) = \mathrm{ESF}(f_x), \quad (3)$$

$$\mathrm{MTF_{total}}(f_x) = \left|\frac{\mathrm{ESF}(f_x)}{\mathrm{STEP}(f_x)}\right|. \quad (4)$$

Considering the direction of MTF, f_x is defined as the spatial frequency along the scanning direction. Considering the impact of over-sampling, Eq. (3) can be discretized as

$$\mathrm{STEP}(f_\mathrm{u}) \cdot \mathrm{OTF}_\mathrm{total}(f_\mathrm{u}) \cdot \mathrm{sinc}\left(\frac{f_\mathrm{u}}{\alpha}\right) = \mathrm{ESF}(f_\mathrm{u}), \quad (5)$$

where f_u is normalized spatial frequency and α is over-sampling coefficient. When differentiating STEP and ESF functions, both sides of Eq. (5) are still equal. But in physical conception, it could be regarded as a point target (differentiation of STEP) passing through imager and generating the corresponding image, namely line-spread-function (LSF). Because of the non-ideal factors, including smoothness and contrast in both sides of knife-edge, the retrieved MTF from Eq. (5) will be with great errors when normalized spatial frequency is larger than 0.2[4]. So, an effective method should be used to retrieve the higher spatial frequency spectrum of MTF.

For an imager on geostationary platform, real applications show that, the most important reason for the decrease of MTF is FPA's slight defocus caused by installation errors and strong shakes during launch. When detectors are placed away from focal plane of optics with a distance of δz, the PSF will be enlarged to a uniform circular area and its diameter is[7]

$$D = \frac{\delta z}{F\#}, \quad (6)$$

where $F\#$ is the F-number of special channel optical system, the unit of δz is in pixel. When neglecting the effect of diffraction, the MTF corresponding to the circular blur area can be expressed as

$$\mathrm{MTF}_\mathrm{total}\left(f_\mathrm{u}\right) = 2 \times \frac{J_1\left(\pi \cdot D \cdot f_\mathrm{u}\right)}{\left(\pi \cdot D \cdot f_\mathrm{u}\right)}, \quad (7)$$

where $J_1(\bullet)$ is the first-order Bessel function. When diffraction of optical system influencing on spatial resolution in some degree, MTF can also be expressed as

$$\mathrm{MTF}_\mathrm{total}\left(f_\mathrm{u}\right) = \begin{cases} \frac{4}{\pi a} \cdot \int_0^{\sqrt{1-(0.5s)^2}} \sin\left[a\left(\sqrt{1-y^2} - s\right)\right] \mathrm{d}y, & s < 1 \\ 0, & s \geq 1 \end{cases}, \quad (8)$$

where $s = \lambda \cdot F\# \cdot f_\mathrm{u}$, and $a = \frac{\pi \cdot f_\mathrm{u} \cdot \delta z}{F\#}$.

It should be indicated that Eqs. (7) and (8) could be used to calculate the lower spatial frequency spectrum with Eq. (5). And, applying the least square error method can get the numerical result of δz. At last, the real imagery spatial resolution could be confirmed by the cut-off frequency of MTF, namely the spatial frequency of the first cross-zero point of MTF.

FY-2C is the first operational geostationary meteorological satellite in-orbit in China. Its main payload is multiple-channel scanning radiator (MCSR), which includes visible, mid-wave infrared (IR), water-wave, and long-wave IR splitter-window channels. Its visible spectrum is between 0.55—0.90 μm and the designed spatial resolution is about 1.25 km at nadir point. To evaluate its real imagery spatial resolution, Australian west coast near the nadir of FY-2C satellite is selected. It should be pointed out that IFOV expressed in angle remains identical during imaging and could be used to calculate the equal image spatial resolution at nadir position with distance between satellite and nadir point[8]. The validation and analysis methods are applied in imageries at different times with the parameters of MCSR and image processing method.

In Fig. 1(a), the lighted dots along coast are selected as knife-edge points, which must be satisfied with which the albedo difference between both sides of knife-edge is larger than 80% of the whole detective range. Clearly, normal directions of the selected points are not the same as the scanning direction (west-to-east). In this meaning, the imagery spatial resolution corresponding to normalized cut-off frequency 0.78 in Fig. 1(d) is in-all-directions, which is larger than that along scanning direction. It is shown from further analysis that, the mean angle between scanning direction and the normal direction of the selected points in this sample is about 32°. So, the equal spatial resolution in scanning direction ($\mathrm{ESR}_\mathrm{scan}$) could be acquired according to the principle of vector decomposition

$$\mathrm{ESR}_\mathrm{scan} = (1.25/0.78) \cdot \cos\left(32°\right) \approx 1.40\ \mathrm{km}. \quad (9)$$

The validation and analyzed results of four main visible detectors' imageries at different time from Nov. 28, 2004 to Dec. 10, 2004 during the in-orbit ground testing of FY-2C satellite are given in Table 1. It can be concluded that, the spatial resolutions of main visible channels Ch1—Ch3 are almost comparative and their means are between 1.45 and 1.48 km. On the other hand, the spatial resolution of the fourth main visible channel (Ch4) is a few lower, about 1.54 km, whose relative error compared with the former is about 3%—5%.

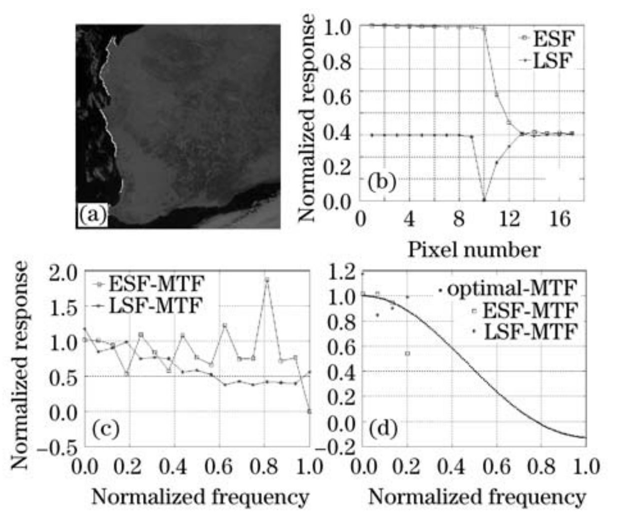

Fig. 1. Imagery spatial resolution retrieval analysis to typical area in FY-2C imageries at time of UTC 08:00 Nov. 9, 2005. (a) Australian west coast imagery; (b) ESF and LSF sketch from (a); (c) coarse MTF from ESF and LSF respectively; (d) optimal MTF with defocused optical model.

Table 1. Equal Imagery Spatial Resolution at Nadir Point Contrast among the Four Main Visible Detectors of FY-2C Satellite

Imaging Time	ESR_{scan} at Nadir Point (km)			
08:00 (UTC)	Ch1	Ch2	Ch3	Ch4
20041128	1.52	1.53	1.42	1.55
20041201	1.45	1.50	1.50	1.40
20041203	1.48	1.34	–	1.58
20041207	1.50	1.62	1.62	1.62
20041208	1.40	1.45	1.53	1.56
20041209	1.34	1.44	1.40	1.54
20041210	1.46	1.51	1.38	1.52
Mean	1.45	1.48	1.48	1.54

When neglecting the effect of algorithm uncertainties, the possible reason is only that the visible detector array was shifted a slight distance toward west, which caused the Ch4 detector to be farther away from the focal plane than the three others. The above conjectural reason is quite similar with that causing stray light difference in imageries among the four visible detectors of FY-2C satellite[9], which is a fair proof in some content to verify the correctness of the analyzed results in Table 1.

In theory, when signal-to-noise ratio (SNR) of system decreases, the imagery spatial resolution will be worsened in some degree. To validate the above conclusion quantitatively, the local imagery of Ch1 detector at UTC 07:00 Nov. 28, 2004 is selected to do some analyses.

It could be concluded from Fig. 2 that, the higher spatial frequency spectrum of MTF free of stray light is more smooth, the normalized cut-off spatial frequency is increased by 0.05 and the corresponding spatial resolution at nadir is also increased by 0.1 to 1.33 km. The results indicate that, stray light not only influences on the SNR of imageries, but also decreases the imagery spatial resolution. So, it should be paid more attention in quantitative applications.

It is pointed out that, the basic start-point of the validation method is to get the system response of a "known" target, retrieve the MTF using characteristics of Fourier optical system, and finally validate the imagery spatial resolution. However, the Australian west coast in Fig. 1(a), is not an ideal step function in mathematics. Hence, there are some errors in the retrieval method. The difference between ideal step function and typical knife-edge function is shown in Fig. 3(a).

Based on the analyzed results to some real imagery, a typical real knife-edge can be considered as a position-extended ideal knife-edge with noise of certain amplitude. To compare different edges' influence on MTF retrieving, the following equation could be inferred from Eq. (3),

$$\mathrm{EDGE}_{\mathrm{true}}(f_{\mathrm{u}}) \cdot \mathrm{OTF}_{\mathrm{total-true}}(f_{\mathrm{u}}) = \mathrm{ESF}(f_{\mathrm{u}}), \quad (10)$$

$$\mathrm{STEP}(f_{\mathrm{u}}) \cdot \mathrm{OTF}_{\mathrm{total-est}}(f_{\mathrm{u}}) = \mathrm{ESF}(f_{\mathrm{u}}). \quad (11)$$

Combining Eqs. (10) and (11), we can obtain

$$\rho = \left|\frac{\mathrm{MTF}_{\mathrm{total-est}}}{\mathrm{MTF}_{\mathrm{total-true}}}\right| = \left|\frac{\mathrm{EDGE}_{\mathrm{true}}(f_{\mathrm{u}})}{\mathrm{STEP}(f_{\mathrm{u}})}\right|. \quad (12)$$

In Eq. (12), ρ is correlation coefficient, illustrated as the dot-line in Fig. 3(b), which represents the relationship between estimated MTF and real MTF. In Fig. 3(b), when normalized spatial frequency is larger than 0.2, the difference between them is quite dissimilar (ρ vibrates greatly in the center of one). It should be said that, normalized spatial frequency of 0.2 here could be regarded as a steady cut-off frequency of the retrieved MTF, which is related to transition and smoothness of knife-edge as well as the number of the knife-edge high-level pixels. Obviously, the error induced by the non-ideal characteristics of knife-edge is the main source of the model.

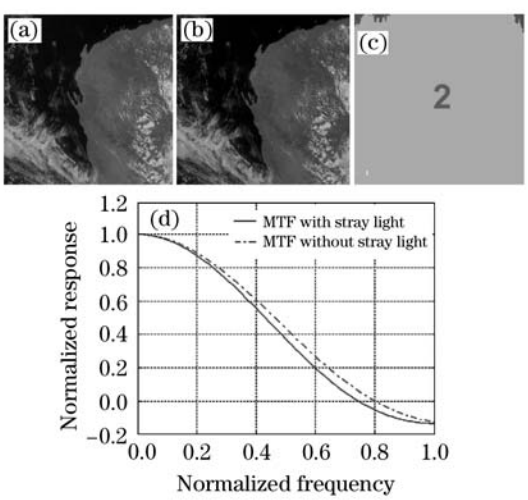

Fig. 2. Analysis of stray light influence on imagery spatial resolution. (a) Imagery with stray light; (b) imagery without stray light; (c) enhanced stray light distribution; (d) MTF contrast between the cases with and without stray light.

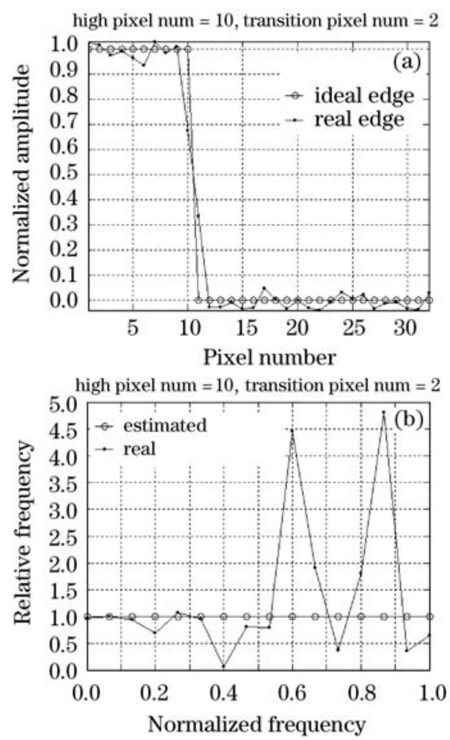

Fig. 3. (a) Contrast between ideal edge and real edge; (b) contrast between MTF estimation distribution and MTF real distribution.

For an imager with a smaller IFOV on geostationary platform, considering the diffraction of optics, the defocused optical models expressed by Eqs. (7) and (8) have the relative same performances. So, the following discussion aims to Eq. (7). Given that the decreasing of MTF is mainly caused by FPA's slight defocus, searching the first cross-zero point of total MTF equals to solving the second cross-zero point of $J_1(\bullet)$. Here, the cross-zero point is marked as zero_2, and from Eqs. (6) and (9),

$$\text{ESR} = \frac{\text{SSR}}{f_\text{u}} \cdot \cos(\theta) = \frac{\pi \cdot \text{SSR} \cdot \cos(\theta)}{\text{zero}_2 \cdot F\#} \cdot \delta z = c \cdot \delta z, \quad (13)$$

where SSR is the standard spatial resolution, θ is the angle between the normal direction of knife-edge and scanning direction, and c is a constant. Clearly, ESR at nadir point is linear to the quantity of FPA's defocus, so the validation accuracy is determined greatly by the fitted accuracy of δz.

When the parameter of $J_1(\bullet)$ is less than 8.0, it can be expressed in the polynomials[10]

$$\begin{cases} J_1(x) = x\frac{C(y)}{D(y)}, \ |x| \le 8.0, \ y = x^2 \\ C(y) = c_0 + c_1 y + c_2 y^2 + c_3 y^3 + c_4 y^4 + c_5 y^5 \\ D(y) = d_0 + d_1 y + d_2 y^2 + d_3 y^3 + d_4 y^4 + d_5 y^5 \end{cases}, \quad (14)$$

where c_i and d_i are constants, $i \in [0, \cdots, 5]$.

Because there are tenth-order nonlinear polynomials about x in Eq. (14), which could not be solved with classical least square method. The tradeoff way is to choose an initial state and look for the optimal defocused distance δz_opm by changing the distance of 1/10 pixel size every step, and the cost function must be satisfied with

$$\text{Error} = \sum_{i=1}^{n} \left[2 \times \frac{J_1(\pi \cdot (\delta z/F\#) \cdot f_\text{u})}{\pi \cdot (\delta z/F\#) \cdot f_\text{u}} - \text{MTF}_\text{total-est}(f_\text{u})\right]^2 \Big|_{\delta z = \delta z_\text{opm}} \to \min, \quad (15)$$

where n is the number of frequency points that is less than normalized cut-off frequency point, and in Fig. 3(b), $n = 4$. For the visible channels of FY-2C satellite, the focal length is about 3000 mm, the diameter of optics caliber is about 400 mm, and IFOV in angle is about 35 μrad. Here, the estimation error of defocused distance will be less than 10 μm, relative error is prior to 3.4×10^{-6} compared with the focal length, so the ESR at nadir point retrieval error will be less than 120 m.

The analyzed results from Fig. 2 show that, imageries of four visible detectors of FY-2C satellite MCSR are affected by stray light, which decreases the system SNR as well as the spatial resolution by about 0.1 km. So, it is very important to retrieve the power distribution of stray light in the whole FOV correctly. But, because of limited accuracy of stray light processing, the residual error is about 2 counts, which will produce 50—100 m error in retrieving ESR at nadir point.

Given the above three errors un-correlation, namely $\rho = 0.9$, the model relative error is 10%. So, the approximate total error of imagery spatial resolution could be estimated as

$$\begin{aligned} &\text{Error}_\text{total} \\ &\approx \sqrt{\text{Error}_\text{model}{}^2 + \text{Error}_\text{fitting}{}^2 + \text{Error}_\text{stray}{}^2} \\ &= \sqrt{(1.25 \times 0.1)^2 + (0.12)^2 + (0.10)^2} = 0.20 \text{ km}. \quad (16) \end{aligned}$$

Drawn from the above analysis and discussions, the precise description of the validation result of imagery spatial resolution at nadir point is: $\text{ESR}_\text{scan} = 1.40 \pm 0.20$ km. Referencing to the designed value of 1.25 km, obviously, the retrieved equal spatial resolution of imager is basically satisfied with the designed requirement. Moreover, considering that the influence of stray light has been alleviated effectively and the ESR could reach 1.33 km, the relative error of the above method is prior to 7%.

Based on the analyses of the main components of imager MTF on geostationary platform, using the special targets' characteristics, the precise evaluation to lower spatial frequency spectrum of system MTF is realized. It is clarified that the main reason that real imagery spatial resolution lower than designed one is FPA's slight defocus. The validation method of visible imagery spatial resolution relying on the defocused optical model and ESF is put forward. The relative error of the method is prior to 7%.

The author wishes to thank for Professor Jianmin Xu for his kindly help to this study. This work was supported by the National Natural Science Foundation of China under Grant No. 40401040. Q. Guo's e-mail address is qiang_g@nsmc.cma.gov.cn.

References

1. S. C. Wu, P. K. Z. Cheng, S. Y. Lee, and A. M. Wu, in *Proceedings of 25th ACRS'2004* PS-5.9, 1638 (2004).
2. L. M. Mugnier and G. Le Besnerais, Proc. SPIE **4483,** 185 (2002).
3. T.-K. Ji and Z.-M. Zhao, J. Remote Sensing (in Chinese) **9,** 486 (2005).
4. J. J. Shea, Proc. SPIE **2812,** 221 (1996).
5. J. J. Shea, Proc. SPIE **3439,** 165 (1998).
6. Q. Guo, J.-M. Xu, and G.-L. Chen, J. Infrared Millim. Waves (in Chinese) **24,** 39 (2005).
7. H. H. Hopkins, in *Proceedings of the Royal Society of London Series A* **231,** 91 (1955).
8. Q. Guo, *Study on the real-time evaluation for the qualities of images of the geostationary meteorological satellites* (in Chinese) Ph.D. Dissertation, Shanghai Institute of Technical Physics, C.A.S. (2003).
9. Q. Guo, J.-M. Xu, and W.-J. Zhang, International Journal of Remote Sensing **26,** 2817 (2005).
10. S. Xu, *Algorithm Programs Group in Common Use* (second edn.) (in Chinese) (Tsinghua University Press, Beijing, 1996) pp.290—294.